Mario Castaño-Álvarez
M. Teresa Fernández-Abedul
Agustín Costa-García

Departamento de Química Física y Analítica,
Universidad de Oviedo,
Asturias, Spain

Received March 2, 2007
Revised April 24, 2007
Accepted April 24, 2007

Research Article

Electroactive intercalators for DNA analysis on microchip electrophoresis

Miniaturized analytical systems, especially microchip CE (MCE), are becoming a promising tool for analytical purposes including DNA analysis. These microdevices require a sensitive and miniaturizable detection system such as electrochemical detection (ED). Several electroactive DNA intercalators, including the organic dye methylene blue (MB), anthraquinone derivatives, and the metal complexes $Fe(phen)_3^{2+}$ and $Ru(phen)_3^{2+}$, have been tested for using in combination with thermoplastic olefin polymer of amorphous structure (Topas) CE-microchips and ED. Two end-channel approaches for integration of gold wire electrodes in CE-ED microchip were used. A 250 μm diameter gold wire was manually aligned at the outlet of the separation channel. A new approach based on a guide channel for integration of 100 and 50 μm diameter gold wire has been also developed in order to reduce the background current and the baseline noise level. Modification of gold wire electrodes has been also tested to improve the detector performance. Application of MCE-ED for ssDNA detection has been studied and demonstrated for the first time using the electroactive dye MB. Electrostatic interaction between cationic MB and anionic ssDNA was used for monitoring the DNA on microchips. Thus, reproducible calibration curves for ssDNA were obtained. This study advances the feasibility of direct DNA analysis using CE-microchip with ED.

Keywords:
DNA intercalators / Electrochemical detection / Gold end-channel detector / Microchip electrophoresis / Topas DOI 10.1002/elps.200700160

1 Introduction

The most promising progress in DNA analysis mainly covers three aspects: conventional and microchip CE (CE and MCE, respectively), MS, and DNA sensors/chips based on the hybridization with oligonucleotide probes.

CE microchips, since they were introduced by Manz *et al*. [1, 2], have demonstrated to be a powerful and useful (bio) analytical tool. These miniaturized systems are characterized by high-speed, high-throughput, small sample, and reagent requirements as well as integration and compactness. Comparing with the relatively mature CE, microchips can be considered as an emerging technology with potential for novel designs and new applications [3].

Microfluidic devices have been mainly fabricated from silicon and glass substrates. However, polymeric materials have been recently used because of their mechanical and chemical properties, low cost, high flexibility, and relatively simple fabrication procedures facilitating mass production of disposable microdevices. Several polymers such as poly(methylmethacrylate) (PMMA) [4], PDMS [5], polycarbonate (PC) [6], polyester [7], and poly(ethylenterephthalate) (PET) [8] have been employed. Recently, cyclic olefin polymers and copolymers such as Zeonor [9] or thermoplastic olefin polymer of amorphous structure (Topas) [10] have also received attention due to their high chemical resistance, good machinability, and optical transparency.

A miniaturized and sensitive detection system is needed for microchip electrophoresis due to the small sample volume. LIF has been commonly adapted to microchips for separation of DNA fragments, genetic analysis, DNA sequencing, and mutation detection as shown in several reviews [11–14]. Nevertheless, this detection system is not yet very compatible with miniaturization and microfabrication technology. Many of the potential benefits associated with miniaturization will be negated if chips must be used in

Correspondence: Professor Agustín Costa-García, Departamento de Química Física y Analítica, Universidad de Oviedo, E-33006 Oviedo (Asturias), Spain
E-mail: costa@fq.uniovi.es
Fax: +34-9-85103125

Abreviations: 2,6-AQDS, 9,10-anthraquinone-2,6-disulfonic acid disodium salt; **1,5-AQDS,** anthraquinone-1,5-disulfonic acid disodium salt; **AQMS,** anthraquinone-2-sulfonic acid sodium salt; **ED,** electrochemical detection; **MB,** methylene blue; **MCE,** microchip CE; **SARS,** severe acute respiratory syndrome; **TBE,** Tris-boric acid-EDTA buffer; **Topas,** thermoplastic olefin polymer of amorphous structure

conjunction with bulky and expensive equipment. Electrochemical detection (ED) provides an alternative of high sensitivity and low cost that can be easily integrated in microanalytical devices due to its inherent simplicity.

In the last years, the conductometric detection mode has experienced an important increase of reporting for analytical [15] and bioanalytical [16] applications including separation of dsDNA and PCR products [17, 18]. However, amperometric detection is the most widely described ED for MCE. A critical step for the good performance of ED in microchips is the cell design for isolation of the detector from the separation electric field. Several approaches have been developed with this aim including in-channel, end-channel, and off-channel configurations.

In- and off-channel detection modes are based on the placement of the working electrode directly within the separation channel without [19, 20] or with an electric field decoupler [21, 22], respectively. The end-channel configuration is the most commonly used amperometric detection mode, where the working electrode is located close (10–50 μm) to the outlet of the separation channel. Different electrode materials and integration/alignment modes have been used for end-channel detectors. The working electrode can be permanently integrated on-chip by means of thin-films made of platinum [23, 24], gold [25–27], copper [26], or carbon [28] placed close to the channel exit. Other approach is based on an off-chip alignment of replaceable disk [10,29–33] or thick-film [33–35] working electrodes. In this case, the working electrode could be replaced when surface fouling happened. Thus, planar thick-film carbon electrodes have been mounted perpendicular to the flow direction [4, 33-35]. Several designs based on a guide tube have been developed in order to align platinum microdisk [31] and carbon fiber [31, 32] electrodes. XYZ micromanipulators have also been employed for aligning metal wire electrodes [8, 29]. Platinum, gold, and copper microwires have been aligned across the separation channel using a channel patterned in PDMS [30].

Electrochemical DNA detection has been commonly accomplished using a label that binds to DNA. Thus, different labels including redox-active molecules [36–39], metal nanoparticles [36], or enzymes [36, 40] have been employed. The simplest mode is based on the use of redox-active molecules which contain a planar aromatic structure that could insert itself between two adjacent base pair of DNA (intercalator) or interact with DNA grooves. In this way, previous labeling of reagents is not necessary and the marker becomes universal. Several metal complexes [36], anticancer agents such as daunomycin [36, 37], organic dyes such as methylene blue (MB) [36–38, 41], and other molecules such as anthraquinone derivatives [36, 42] have been used as intercalators and groove binders.

In the development of integrated DNA analysis systems an area where improvements are needed is that of product detection [11]. Obtaining an adequate signal for DNA strands is a key step for developing an appropriate methodology. Amperometric detection has been also used in combination with MCE for DNA analysis. Redox indicators of DNA have been widely employed in biosensors for monitoring DNA hybridization [43, 44]; however, bibliography related to the employ of indicators with the aim of detecting DNA in CE microchips is scarce when ED is concerned. A laborious covalent labeling of allele-specific primers with ferrocene has been performed for a PCR-based SNP typing assay employing CGE on microchip [27]. This molecule is employed also as label for chain terminators in the detection of SNPs by CGE microchip in a single-base extension reaction [28]. Apart from this covalent labeling, an indirect ED through the complex $Fe(phen)_3^{2+}$ that acted as intercalation agent has been developed to separate and detect DNA restriction fragments and PCR products [23, 27] on CGE microchips. The constant background current from free $Fe(phen)_3^{2+}$ in the separation buffer decreases when DNA- $Fe(phen)_3^{2+}$ complexes migrate through the detection region, so the passage of DNA is indicated by transient dips in the background current. This is the first time, to the best of our knowledge, that specific interaction of an intercalator with ssDNA is electrochemically detected on a CE microchip.

Thus, in this work, several electroactive DNA intercalators have been evaluated for their possible application on CE-microchips. Taking into account the significance that this miniaturized detection is achieving is relevant the consecution of a suitable signal. The use of noncovalently bound probes eliminates the need for previous chemical modification avoiding additional preparative tasks and decreasing analysis time. In this case, the amperometric detection on Topas-microchip has been achieved using two different end-channel approaches based on gold wire electrodes of various diameters. Modification of the gold electrodes has been also tested in order to improve analytical signals. Optimal detection system in combination with the Topas-microchip has been employed for ssDNA analysis using the electrostatic interaction with an electrochemical indicator. The sequence is complementary to one specific to the severe acute respiratory syndrome (SARS)– associated coronavirus, the causative agent of an outbreak of atypical pneumonia.

2 Materials and methods

2.1 Reagents

MB, 9,10-anthraquinone-2,6-disulfonic acid disodium salt (2,6-AQDS, 98% purity), anthraquinone-1,5-disulfonic acid disodium salt (1,5-AQDS, 95% purity), anthraquinone-2-sulfonic acid sodium salt (AQMS, 97% purity), dichloro tris(1,10-phenanthroline) ruthenium (II) ($Ru(phen)_3^{2+}$), 1,10-phenanthroline iron(II) sulfate complex ($Fe(phen)_3^{2+}$), Tris, 1-hexanethiol (95%), L-cysteine (L-Cys), SDS, and boric acid (99.5%) were purchased from Sigma–Aldrich (St. Louis, MO, USA). EDTA was supplied by Fluka (Buchs, Switzerland). Potassium chloride, perchloric acid (70%), and ethanol were obtained from Merck (Darmstadt, Germany).

A synthetic 30-mer ssDNA with sequence 5'-CTT TTT CTT TTT GTC CTT TTT AGG CTC TGT-3' was purchased from Eurogentec (Belgium). This sequence is complementary to the portion of the SARS genome [45] comprised between bases 29218 and 29247, both included. Oligonucleotide solutions were prepared in TE buffer pH 8.0 (0.1 M Tris-HCl buffer solution, 1 mM EDTA). Aliquots were prepared and stored at –20°C. Working solutions of ssDNA were prepared from aliquots in the running buffer and conserved at 4°C.

All other solutions were prepared in the running buffer and filtered through nylon syringe filters (Cameo 30N, 0.1 μm, 30 mm) obtained from Osmonics (Minnetonka, MN 55343, USA).

Water was purified employing a Milli-Q plus 185 equip from Millipore (Bedford, MA 01730). All other reagents were of analytical reagent grade.

2.2 Microchip design

Topas (thermoplastic olefin polymer of amorphous structure) microchips, shown in Fig. 1. I, were purchased from Microfluidic-ChipShop (Jena, Germany). Microchips consisted of a plate (58.5 mm × 13.5 mm) of 2 mm thickness with a 54 mm long separation channel (between the running buffer reservoir, A, and the waste/detection reservoir, B) and 9 mm long injection channel (between the sample reservoir, C, and the sample waste reservoir, D). The two channels crossed each other halfway between the sample (C) and sample waste (D) reservoirs and 4.5 mm from the separation channel buffer reservoir (A). An additional 4.5 mm channel (E) was placed at 4.5 mm from the end of the separation channel. The channels were 20 μm depth with 32 μm width at the bottom and 60 μm width at the top. A cover plate of similar dimensions but 200 μm thickness is adhered for closing the channel at the top. Holes of 2 mm diameter that act as reservoirs were situated on the 2 mm thick plate at the end of the channels. Micropipette tips were cut for obtaining 1 cm long pieces with a diameter of 0.5 cm at the top. They were adhered concentrically to the chip holes with Araldit (Vantico AG, Basel, Switzerland) forming reservoirs of approximately 100 μL volume. A methacrylate holder (18 cm × 13 cm × 2 cm) was fabricated for accommodating the chips. Once inserted the chip on the holder, a small rectangular piece (5 cm × 1 cm × 0.8 cm) was fixed with screws with the aim of securing the chip.

2.3 Electrochemical detector

The amperometric detector was situated in the waste reservoir (B) with a three-electrode configuration. The reference and counter electrodes were coupled in a 250 μL micropipette tip that was introduced in the detection reservoir for performing the measurements. The reference electrode consisted of a 1 mm diameter silver wire (Goodfellow, UK) anodized in saturated KCl and introduced in a pipette tip through a syringe rubber piston. The tip was filled with saturated KCl solution and contained a low-resistance liquid junction. The auxiliary electrode, a 0.3 mm diameter platinum wire (Goodfellow), was externally fixed with insulating tape. Gold wires (Alfa Aesar, Germany) with different diameters (250, 100, and 50 μm) were used as working electrodes with an end-channel configuration.

The 250 μm diameter gold wire working electrode was manually aligned at the outlet of the separation channel as previously reported [10]. In brief, the wire was introduced in the reservoir with the aid of a micropipette tip, then, it was

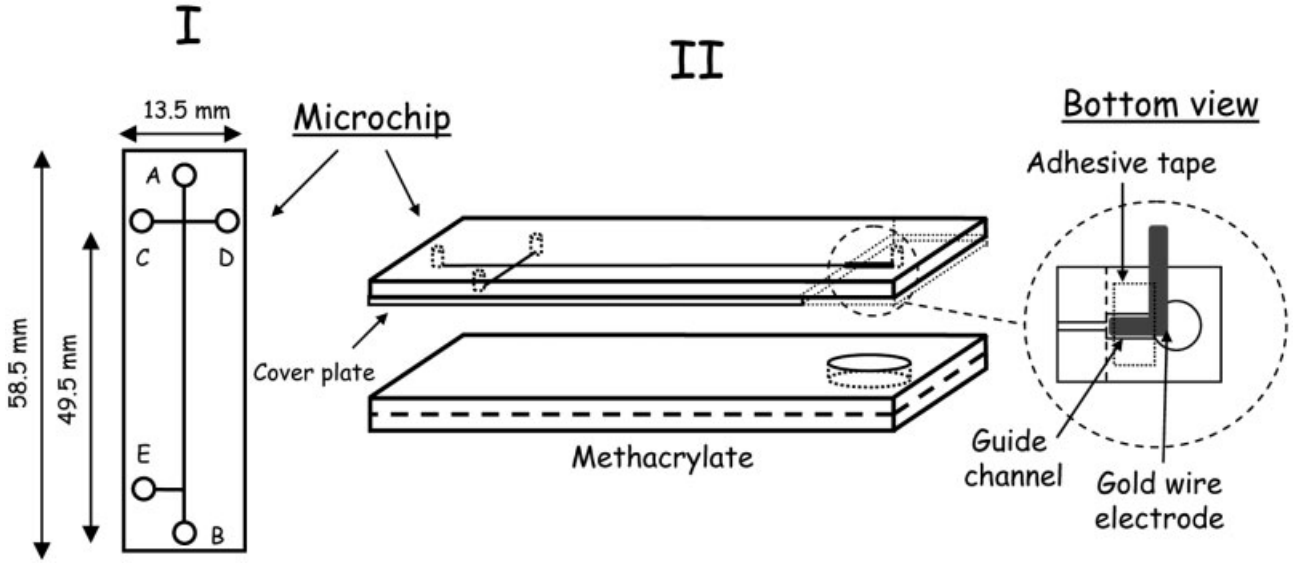

Figure 1. Microchip (I) and amperometric detector (II) design.

adhered to the microchip with Araldit. Finally, a 1 cm long piece of a 250 μL micropipette tip was adhered to the chip hole fixing the wire.

A new end-channel detector design was developed in order to align the 100 and 50 μm diameter gold wire electrodes (Fig. 1.II). A part of the cover plate was removed, leaving open the last part of the separation channel (approximately 1 mm). The open channel was widened with a cutter in order to obtain a guide channel of appropriated dimensions for aligning accurately the 100 and 50 μm diameter electrodes. The gold wire was coupled to a piece of adhesive tap (1 mm approximately) for allowing easier handling and was placed and aligned in the new guide channel with the aid of a microscope (Swift Optics, USA). The electrode was fixed on the guide channel with epoxy resin (Araldit) and adhesive tape. After the glue was cured, the wire was turned 90° at the end of the adhesive tape and was also fixed with epoxy resin. In this way, the gold wire is in contact with the solution only at the end of the channel and not in the rest of the reservoir, which could increase capacitive currents. The microchip was joined to a methacrylate block consisting of two pieces. In the one that contacts the microchip, a circular cavity (5 mm diameter and 2 mm deep) that includes the initial 2 mm diameter hole, was practiced in order to make the final detection reservoir. All the pieces were maintained together with Araldit. Finally, a copper cable was fixed to gold wire with a conducting silver epoxy resin (CW2400, RS Components, UK) for electrical connection.

Cyclic voltammetry experiments were carried out using the waste/detection (B) reservoir as electrochemical cell. A 250 μm diameter gold wire was employed as working electrode. The tip containing the reference and auxiliary electrodes was also introduced in the reservoir for performing the measurements. Alternatively, a card with screen-printed electrodes and electrical carbon connection (Alderon, USA) was modified [33] and employed for performing cyclic voltammetry experiments.

Amperometric and cyclic voltammetric detection was performed with an Autolab PGSTAT 10 (ECO Chemie, Netherlands) potentiostat interfaced to a Pentium Celeron, 333 MHz, 64 MB RAM computer system and controlled by Autolab GPES software version 4.9 for Windows 98.

2.4 Electrophoresis procedure

CZE separations were carried out in uncoated channels using two high-voltage power supplies (HVPS, MJ series) with a maximum voltage of +5000 V from Glassman High Voltage (High Bridge, NJ 08829-0317, USA). They were interfaced to a Pentium Celeron, 333 MHz, 64 MB RAM computer system and monitored by a DT300 Series Board, DT Measure Foundry 4.0.6 software for Windows 98. High-voltage electrodes consisting of 0.3 mm diameter, 1 cm long platinum wires (Goodfellow) were inserted into each of the reservoirs and connected by means of crocodile clips to the HVPS.

Prior to electrophoresis, Topas microchips were rinsed with 0.1 M $HClO_4$ and running buffer for 15 and 10 min, respectively. Washing was made with the aid of a simple vacuum system and reservoirs were filled with the running buffer solution. The microchip was fixed in its holder and a Faraday cage was used for housing it in order to minimize electrical interferences. After baseline stabilization, reservoir C was filled with the sample solution and injections were performed by applying the desired voltage. Several types of injections ("pinched" and "unpinched") were evaluated. Separation was performed by applying the corresponding voltage (usually +2000 V) to the running buffer reservoir (A) with the detection reservoir (B) grounded. Then, the detection potential was applied and the electropherogram was recorded. All experiments were performed at room temperature.

Safety considerations: High-voltage power supplies should be handled with extreme care to avoid electrical shock.

3 Results and discussion

3.1 Electroactive DNA intercalating ligands

Although DNA can be detected through label-free approaches by monitoring the oxidation or reduction current of electroactive bases [44, 46], electrochemically active intercalators have been widely employed in the development of genosensors [43, 44]. The process of guanine, the most oxidizable base, occurs at highly positive potential (around +1.0 V *vs.* Ag/AgCl) and background currents are high. Moreover, species in biological samples may be oxidized causing a positive error. Addition of an indicator molecule improves the detection with a simple procedure. As commented in the introduction, the use of intercalators is common in sensors but there is not reference of their specific use in CE microchips. In this work, the organic cationic dye MB, the organic anionic species including 2,6-AQDS, 1,5-AQDS, and AQMS, as well as metal complexes such as $Ru(phen)_3^{2+}$ and $Fe(phen)_3^{2+}$ have been evaluated by cyclic voltammetry using a 250 μm diameter gold wire electrode. TBE buffer (50 mM Tris-boric acid pH 7.0, 1 mM EDTA) was used as BGE in all studies. Solutions of anthraquinones have to be degassed with nitrogen for 10 min in order to avoid the interference of the oxygen signal.

Anthraquinone derivatives have been described as redox intercalators with long-range electron transfer (LET) through dsDNA [42, 47] immobilized on a sensor surface. A single strand of probe DNA will not allow efficient LET to occur and the free surface is blocked to avoid direct transfer. From the several anthraquinone derivatives, three among them: the monosulfonic (AQMS) and two different disulfonic (2,6-AQDS and 1,5-AQDS) were evaluated. The cyclic voltammogram recorded in a 1 mM AQMS solution is shown in Fig. 2A. A cathodic process that appears at −0.662 V corre-

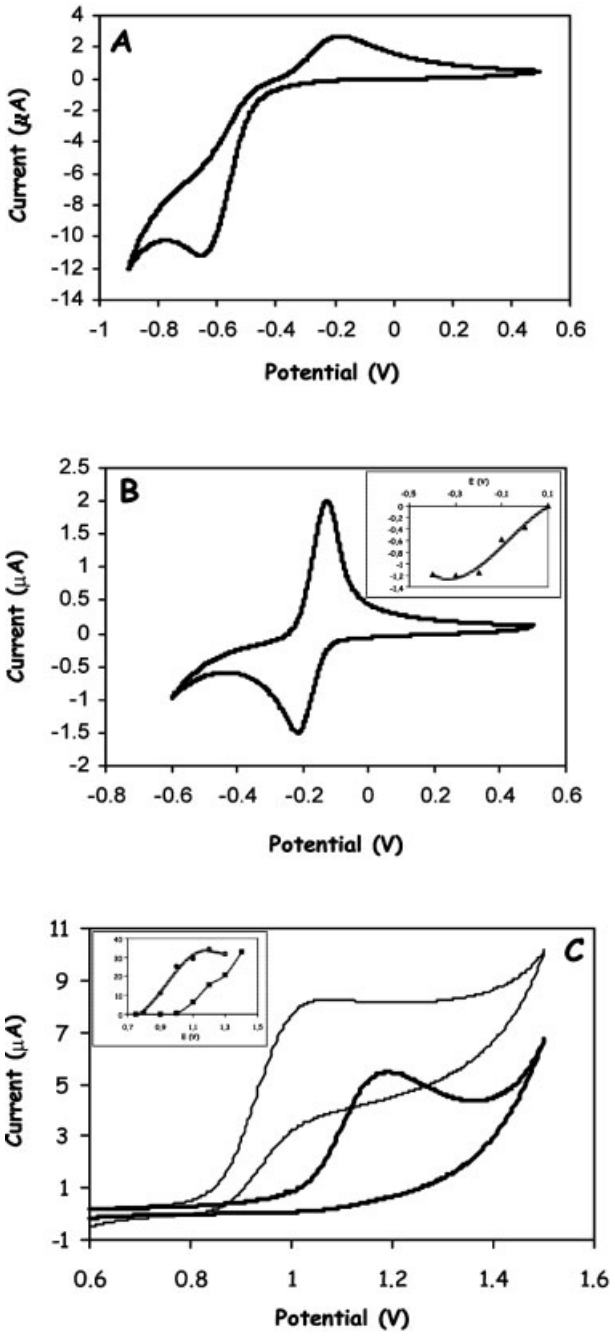

Figure 2. Cyclic voltammograms with a gold wire electrode for (A) 1mM AQMS, (B) 100 μM MB, and (C) 145 μM $Fe(phen)_3^{2+}$ (—) and 100 μM $Ru(phen)_3^{2+}$ (▬) using TBE buffer and v = 50m V/s. (Inset: hydrodynamic voltammograms for MB (▲), $Fe(phen)_3^{2+}$ (●), and $Ru(phen)_3^{2+}$ (■) using a Topas-microchip with a 250 μm gold wire detector. Conditions: V_{sep} = +2000 V; injection: 5 s at +2000 V; running buffer: TBE

sponds to the reduction of the keto groups of the antraquinone to the corresponding alcohol. The reoxidation to the keto form occurs at −0.137 V. When the voltammogram is recorded in a 2,6-AQDS solution, the redox process becomes poorly defined and the closeness of the background current makes difficult the measurement of cathodic currents. When the two sulfonic groups are in a nearer position (1,5) the process becomes more irreversible. The amperometric detection of antraquinones will require an optimal detection potential over –0.5 V, where solutions must be deareated. Since moreover, this potential is near the background current, it will increase the baseline noise level. Therefore, anthraquinone species were discarded for DNA application on MCE. In addition, these molecules possess sulphonic groups and therefore they are negatively charged at the working pH and could suffer repulsion from polyanionic DNA.

MB is a common intercalator dye that presents a well-defined reversible redox process as can be seen in Fig. 2B. The cyclic voltammogram shows a cathodic process at −0.215 V (conversion of MB to leucomethylene blue (LB), a two electron process [38]). The corresponding anodic process appears at −0.127 V which means a difference of 0.088V ($i_{p\,an}/i_{p\,cat}$ = 1.37). In both cases, the peak current varies linearly (r equal to 0.9996 and 0.998 for the anodic and cathodic processes, respectively) with the square root of the scan rate, indicating that the processes are diffusion controlled. The precision of the signals is very adequate since where ten measurements are successively recorded, an RSD of 3.0 and 3.1% is obtained for the oxidation and reduction processes, respectively. The process was also checked at carbon electrodes (screen-printed electrodes). Although it becomes more reversible (ΔE = 0.056V, $i_{p\,an}/i_{p\,cat}$ = 1.03) the intensity of successive signals is increasing with the number of the scans. The third signal is 3.1 ± 0.3 times higher when compared with the first one, which implies the necessity of performing an electrode pretreatment for obtaining reproducible signals. Activation procedures are usual when solid electrodes are used but when they are part of a microchip the whole procedure becomes more complicate and the performance of the detector can deteriorate. Moreover, the intensities of the peak current are always lower than those obtained with gold wires for the same MB concentration (10 μM). Therefore, the process that MB presents at gold electrodes seems to be more adequate for following the signal of DNA. MB has been shown to bind specifically to the guanine bases of ssDNA [48, 49]. Furthermore, as MB is positively charged, its interaction with DNA is easier and more rapid than for anionic intercalators.

Both processes, oxidation and reduction, are appropriate but since MB has first to be reduced to LB if oxidation want to be observed, the amperometric procedure will imply the application of a cathodic potential before fixing the anodic. Therefore, for the sake of simplicity, the cathodic process has been chosen. In order to determine the optimum detection potential, a hydrodynamic voltammogram has been recorded using a Topas-microchip with a 250 μm diameter gold wire electrode. A separation voltage of +2000 V (370 V/cm), an injection voltage of +2000 V applied for 5 s and TBE as running buffer was employed. The potential was varied between

+0.1 and –0.4 V. The intensity is increasing and reaches a plateau at –0.2 V (Fig. 2B, shown as inset). A potential of −0.3 V was employed as working potential to detect the MB reduction process on CE-microchip.

Synthetic organic molecules [50] have been prepared for intercalators. Similarly, metal complexes have been synthesized in order to improve the analytical signal since the interaction between the complexes and DNA varied significantly depending on the nature of ligands. In this work, only commercial products have been checked: $Ru(phen)_3^{2+}$ and $Fe(phen)_3^{2+}$. They were both employed as DNA groove binders and intercalators [51, 52]. The ligand 1,10-phenantroline (phen) possesses three aromatic rings and when it is compared with other polypyridyl ligands in cobalt complexes, it results to be the most electrochemically reactive [53]. $Ru(phen)_3^{2+}$ and $Fe(phen)_3^{2+}$ showed an irreversible oxidation process at +1.2 and +1.0 V, respectively (Fig. 2C). Hydrodynamic voltammograms performed in the microchip with conditions similar to those employed for MB are included as an inset. They reached a plateau at +1.3 and +1.1 V, respectively. In the case of $Ru(phen)_3^{2+}$ the background current is very close to the process and can difficult the detection. Both require a high detection potential that can affect the good performance of the detector. Therefore, these metal complexes have been discarded and only MB was used in the remainder of the work.

3.2 Microchip performance

Once the indicator molecule has been chosen, the analytical signal of the electroactive dye, MB, in the MCE with end-channel gold wire detection was checked. Obtaining an adequate signal is of paramount relevance in order to monitor the interaction with DNA. Several parameters, such as injection mode and detection system, that could affect the good performance of microchip, were evaluated.

A Topas-microchip with a 250 μm diameter gold wire electrode was initially used to monitor the MB reduction. Fig. 3A shows the amperometric signal of a 100 μM MB solution on Topas-microchip with a separation voltage of +2000 V, an injection voltage of +2000 V applied for 5 s, TBE as running buffer and −0.3 V as detection potential. Since MB is a cation at the working pH it should appear before the EOF. This means that the migration time is going to be lower than this of other neutral or anionic intercalators. Under the conditions stated above, the migration time for MB is around 40 s. The intensity at the maximum of the peak is −5nA. Although the front of the peak is marked, an excessive band broadening was observed. Indeed, the peak did not turn back to the baseline until 100 s approximately. Moreover, the baseline current with the 250 μm diameter gold wire was relatively high (−24 nA) as well as the noise level (0.2 nA), which could pose a problem when sensitivity is required. This is probably due to the area of the gold wire electrode. Taking into account the design of the chip detection, only the gold area in front of the microchannel outlet is

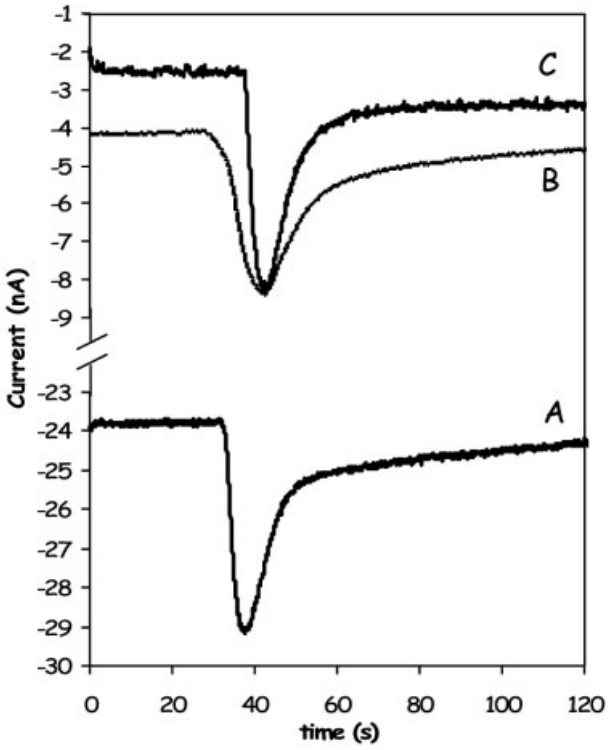

Figure 3. Electropherograms for 100 μM MB at 250 μm gold wire electrode unmodified (A) and modified with L-cysteine (B) and 1-hexanethiol (C). Conditions: running buffer, TBE; V_{sep} = +2000 V; injection: 5 s at +2000 V; E_d = –0.3 V (*vs.* Ag/AgCl).

responsible for analytical signals. However, as the working electrode is a wire, the rest of the area of the electrode could contribute to the capacitive current that is proportional to the electrode area, increasing band broadening, and noise level.

Electrode modification with self-assembled monolayers (SAMs), especially on gold materials, is being commonly employed in order to improve analytical signals [54–57], intervening for instance in ion binding, protein adsorption, or surface blocking. Mercaptohexanol has been employed for prevent AQDS from undergoing direct electrochemistry [42] and 1-hexanethiol was employed for minimizing nonspecific adsorption at gold surfaces, which produced moreover a decrease in the charging current [58]. In this case, modification of the electrode with 1-hexanethiol and L-cysteine was studied in order to decrease the background current and the baseline noise level.

The detection reservoir (B) where the gold working electrode is located was filled with a solution of 1-hexanethiol 2% v/v in ethanol. After 30 min, the solution was replaced by the running buffer (TBE) and electropherograms of MB were recorded. Figure 3C depicts the electropherogram obtained for 100 μM MB at 1-hexanethiol modified gold wire electrode. A decrease in the background current was observed (−2.5 nA) without prejudicing the intensity (−5 nA). How-

ever, better noise level was not obtained. Nevertheless, a little improvement of the peak shape was shown with a decrease of the half-peak width ($w_{1/2}$). When the incubation time of 1-hexanethiol was increased, a decrease in the peak current was observed which demonstrates that it acts as a surface blocking agent that prevents electrochemistry. Thus, when the gold electrode was incubated with 1-hexanethiol overnight, analytical signals of MB were suppressed. This indicates that the gold area in front of the channel outlet becomes covered by the alkanethiol.

Similarly, the gold electrode was modified with a 1 mM L-cysteine aqueous solution. In this case, after 30 min of interaction, a slight decrease on the noise level was shown. Although the background current remains low, a decrease in the peak current and increase in the half-peak width is produced as can be seen in Fig. 3B.

A calibration plot for MB was performed using 1-hexanethiol modified gold wire electrode on Topas microchip. A linear range comprised between 0.5 and 200 μM with a sensitivity of 54 pA/μM and a correlation coefficient of 0.9993 (n = 7) was obtained. The LOD for MB was 0.3 μM (S/N = 3).

The precision was also evaluated from a series of repetitive injections of a 100 μM MB solution. The RSD of the peak current for 12 successive signals was 2.1% ($i_{p\ (average)} = -5.4$ nA). The RSD of the migration time was 2.4% ($t_{m\ (average)}$ = 38.6 s). This is very adequate if an absence of electrochemical pretreatment for the solid electrode is considered. Moreover, the channel is initially conditioned but no special treatments are made between runs.

On the other hand, an alternative to improve the analytical signal of MB with a better S/N was the employ of gold wires with smaller diameter. Considering the geometry of the microchannel, 20 μm depth with 32 μm width at the bottom and 60 μm width at the top, the 250 μm diameter gold wire covers the entire outlet. MB reaches the electrode frontally and gives a sharp peak but then it continues along the electrode wall meanwhile it dilutes, producing band broadening. Thus, 100 and 50 μm diameter gold wire were checked as working electrode in combination with Topas microchips.

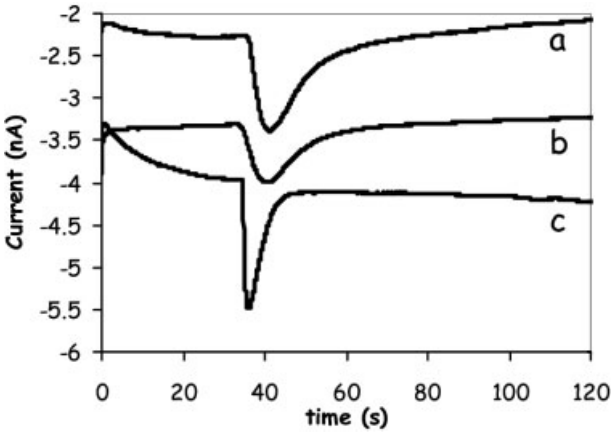

Figure 4. Electropherograms for 100 μM MB at gold wire electrode with 50 μm diameter (a) and 100 μm diameter with a channel-to-electrode distance of >100 μm (b) and <50 μm (c). Conditions as in Fig. 3.

Figure 4 presents the electropherograms for 100 μM MB using different diameter gold wire electrodes and Table 1 shows a comparative of parameters such as peak current (i_p), half-peak width ($w_{1/2}$), background current, noise level, and S/N for the different gold wire electrodes. Although the peak current of MB with 100 and 50 μm diameter gold wire was lower than this for 250 μm diameter, the noise level was also lower, approximately ten times lower. Thus, S/N was approximately two-fold higher in those for the same MB concentration. This increase was probably due to the smaller area of the electrode and the lowest effect of the high voltage.

The distance between the working electrode and the outlet of the separation channel is another parameter that affect the analytical signal [24, 27, 31, 32, 59]. This is clearly seen in Figs. 4b and c, where electropherograms recorded employing a 100 μm diameter gold wire located at different distances from the channel exit are presented. When the electrode was too far from the channel outlet (more than 100 μm, Fig. 4b) a decrease in the intensity was observed due to analyte dilution in the reservoir. It can also be noted that

Table 1. Comparison of parameters for different gold wire electrodes

	Gold wire electrode				
	250 μm ∅ Bare	250 μm ∅ Hexanethiol	250 μm ∅ L-Cysteine	100 μm ∅	50 μm ∅
i_p (nA)	−5.4	−5.6	−4.2	−1.5	−1.1
$w_{1/2}$ (s)	12.5	9.5	16.2	4.5	8.5
Background current (nA)	20–40	0–10	0–10	0–10	0–10
Noise level (nA)	0.2	0.2	0.15	0.025	0.020
S/N	25	25	25	60	55

Conditions: 100 μM MB, separation: +2000 V, injection: +2000 V at 5 s, detection potential: −0.3 V, TBE buffer.

the peak is not as sharp in the front as before. Meanwhile, if the electrode was closer to the separation channel (below 50 μm, Fig. 4c) an increase in the peak current is observed. In this case, a slight initial baseline slope, due to the influence of high voltage, reflected the proximity of the electrodes to the outlet. A very small channel-to-electrode distance could result in relatively intense interference of the separation voltage on the detection, decreasing the sensitivity too. Therefore, selecting an appropriate distance can ensure effective hydrodynamic transport of the analyte zone toward the electrode surface and minimize the influence of the high electric field.

Modification of the 100 μm diameter gold wire with 1-hexanethiol was also tested. However, in this case, better S/N was not obtained. Thus, unmodified 100 μm diameter gold wire electrode was employed in the remainder of the work due to its better S/N as well as the easier and more accurate alignment when compared to that of 50 μm diameter.

Using this working electrode with Topas microchips, the influence of the injection in the analytical signal of MB was studied. Band broadening could also be due to the sample plug shape and therefore the injection format could influence it. Thus, two different approaches of unpinched and a special pinched injection have been evaluated.

In the first unpinched injection, the positive connection was situated in the sample reservoir (C), while the sample waste reservoir (D) and the detection reservoir (B) were grounded. Hence, high voltage was applied between C and D/B reservoirs. In the second unpinched injection, the positive connection was also situated in C reservoir, but only the detection reservoir (B) was grounded. Thus, high voltage was applied between C and B reservoirs. In both cases, an injection voltage of +1500 V was employed and a time control (between 5 and 10 s) of the high voltage was needed in order to improve the sample plug. After the unpinched injection, the separation voltage (+2000 V) was applied between A and B reservoir without push-back voltage on C and D reservoir. Although similar peak shapes were obtained with both unpinched injections (data not shown), the second one increased slightly the peak current and the half-peak width due to the increase in the sample volume injected because the sample will go preferentially to B. When the injection time was increased from 5 to 10 s, an increase in the peak current was also shown. However, an excessive half-peak width (>15 s) was also observed which affects to resolution on separations. This effect was more notorious in the second unpinched injection, which requires a better injection time control.

In the pinched injection, the positive connection is located in the sample reservoir (C) with the sample waste reservoir (D) grounded, and a push-back positive voltage should be applied in A and B reservoir in order to avoid the leakage of the sample into the separation channel [60]. However, as the detector electrodes are in B reservoir, no voltage can be applied in it. Thus, in order to apply the push-back voltage an additional reservoir (E) was employed. After injection, the separation voltage (+2000 V) was applied between A and B reservoir with a push-back voltage on C and D reservoir. In E reservoir nonvoltage was applied. Various push-back voltages, +250, +500, and +1000 V, were evaluated with an injection voltage of +1500 V applied for 5 s. When this pushing voltage was increased, a lower half-peak width was observed. Thus, the peak width decreased from 11.1 to 8.6 s when it moved from +250 to +1000 V, respectively, probably due to a reduction in the sample volume injected. However, a decrease in the peak current as well as a higher initial baseline slope was shown, which means that the pushing voltage during the separation also affected the detector.

Although pinched injection allows a better control of the sample plug, the second unpinched injection with a voltage of +1500 V applied for 5 s was employed in this work due to its simplicity as well as a better compromise between peak current and half-peak width.

A calibration curve for MB is performed with this system (unpinched injection at +1500 V for 5 s with a separation voltage of +2000 V and a detection potential of −0.3 V in a 100 μm gold wire working electrode) employing a 50 mM Tris-boric buffer pH 7.0 (the change in the buffer composition is explained in next section). A linear relationship is obtained between 0.25 and 200 μM MB with a slope of 33 pA/μM ($r = 0.996$, $n = 8$). The LOD in this case is 0.2 μM.

The precision of the measurements resulted to be 2.1% in terms of RSD for ten successive injections of a 100 μM solution with an average peak current of −2.5 nA. The RSD for the migration time is 2.4% (average of 43.5 s).

3.3 DNA application

DNA analysis plays an important role in genetic, medical research, and clinical diagnosis. Development of new methods using CE microchips could become a powerful bioanalytical tool for high-throughput DNA analysis. Up to now, CE-microchips with amperometric detection have not been widely employed for DNA analysis. However, electrochemically active indicators can be successfully used for DNA detection on microchips. This is the first time that the interaction between one of these molecules, MB, and ssDNA is demonstrated in a CE microchip.

A 30-mer ssDNA with a specific sequence of SARS coronavirus has been directly labeled with the electroactive intercalating dye MB for ED on Topas-microchips. MB has been supposed to interact with guanine base of DNA [48, 49], which is also attended by the electrostatic attraction between the cationic MB and polyanionic DNA. In this case, four guanine bases are present in positions 13, 23, 24, and 29, that can interact with MB.

Labeling reaction of ssDNA with MB was developed off-chip so that, the mixture of ssDNA, MB, and ssDNA-MB complex was injected on microchip. The reaction was performed adding DNA to dye as previously reported [61]. This mixing order was determined to affect the distribu-

tion of dye molecules on DNA fragments. Moreover, in this way, a signal of MB before interaction with ssDNA can be obtained.

Figure 5 shows the electropherograms recorded for the sample mixture of 100 μM MB and 10 ng/μL ssDNA as well as single 100 μM MB on a Topas-microchip using a separation voltage of +2000 V (370 V/cm), an injection voltage of +1500 V applied for 5 s and TBE as running buffer. In Fig. 5A, the signal corresponding to a MB solution is shown. When ssDNA is added, two peaks were initially recorded (Fig. 5B), the first one, at 40 s, corresponding to free MB and the second one, at 80 s, was due to ssDNA-MB complex. DNA is not electroactive at this potential and therefore this signal must be due to MB associated to DNA. Moreover, DNA, as a polyanion, moves against the direction of EOF. The mobility of DNA would be smaller than that of free MB and EOF. Although charges can be partially compensated by MB, it appears separately at higher times accordingly to its charge/mass ratio. The separation efficiency, expressed as the theoretical plate number (N), was 8700 ± 500 and 29 000 ± 2000/m for free MB and ssDNA-MB complex, respectively. An excellent resolution ($R_s = 4$) was also shown. Nevertheless, the second peak was not very reproducible with time and sometimes it could even disappear.

Various modifications of the running buffer were studied in order to stabilize the signal for the ssDNA-MB complex. Thus, SDS was added to the initial running buffer TBE (50 mM Tris-boric acid pH 7.0, 1 mM EDTA) in a 1 mM concentration, that is below the critical micellar concentration. When this buffer was employed, a decrease on the analytical signal of MB was observed. Additionally, nonsignal of ssDNA-MB was observed. Since SDS is an anionic surfactant, it can interact with cationic MB and probably impede the interaction with ssDNA. Actually, MB has been employed for the spectrophotometric determination of surfactants since they form an ionic pair that can be extracted in chloroform [62].

On the other hand, a decrease in the ionic strength of the running buffer was also tested in order to improve the interaction ssDNA-MB. Since ssDNA possesses phosphate groups that render it anionic, ions from the solution may interact with them and impede its interaction with MB. Moreover, in the modes of binding of MB the influence of the ionic strength is of relevance [63]. Thus, TB buffer (50 mM Tris-boric acid pH 7.0) without EDTA was employed. EDTA could interact with MB and interfere its interaction with ssDNA. In this case, a slight increase on the free MB and ssDNA-MB peak current is seen. However, the ssDNA-MB signal disappears with time.

Using TB buffer, 10 ng/μL of ssDNA was added to different MB concentrations (25, 50, and 100 μM). Quite similar signals for the ssDNA–MB complex were obtained, meanwhile, important differences were found for the single MB signal. A decrease in the initial MB signal was observed after mixing with ssDNA, that was more important when MB concentration decreased. Even, the signal for 25 μM MB almost disappeared completely after adding 10 ng/μL of DNA. Taken into account it, a MB concentration of 50 μM was used for the rest of the studies with ssDNA.

Since analytical information could not be obtained from the signal of ssDNA–MB complex, the signal of free MB was studied in order to acquire analytical information from DNA. Different DNA concentrations (0.5, 1, 5, 10, 20, and 40 ng/μL) were added on 50 μM MB aliquots and the resulting solutions were measured on the Topas-microchip just after mixing. The analytical signal corresponding to the MB reduction significantly decreased upon addition of DNA (Fig. 6). The peak current of MB decreased with a rate of 2% *per* ng/μL of DNA. Thus, a calibration plot based on the decrease of MB peak with the ssDNA was found to be linear in the range 5–40 ng/μL with a sensitivity of 31 pA μL/ng ($r = 0.998$, $n = 5$). The LOD estimated was 4 ng/μL, corresponding to a mass of 0.4 pg in a 100 pL sample injection.

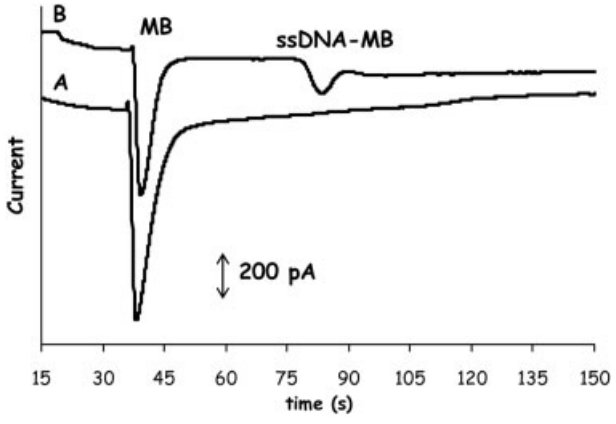

Figure 5. Electropherograms for (A) 100 μM MB and (B) a mixture of 100 μM MB and 10 ng/μL ssDNA using a Topas-microchip with a 100 μm gold wire detector. Conditions: running buffer: TBE, V_{sep} = +2000 V; injection: 5 s at +1500 V; E_d = −0.3 V (*vs.* Ag/AgCl).

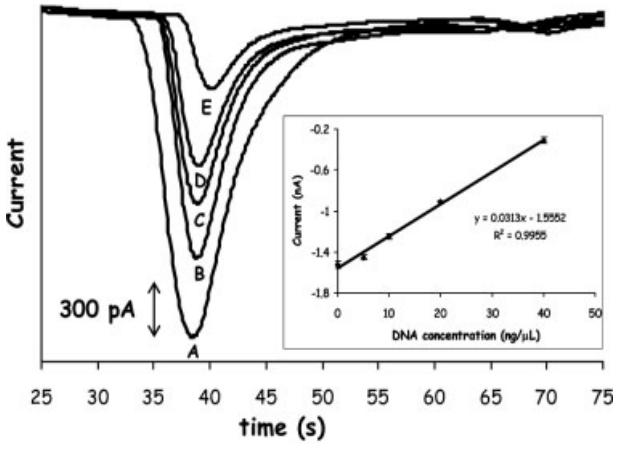

Figure 6. Electropherograms for mixtures of 50 μM MB with increasing levels of ssDNA: (A) 0, (B) 5, (C) 10, (D) 20, and (E) 40 ng/μL. The resulting calibration plot is shown as inset. Conditions: running buffer: TB; other as in Fig. 5.

This was calculated as the concentration corresponding to a decrease in the signal that is three times the SD of the blank (signal of free MB without adding DNA).

The precision of the labeling reaction of DNA with MB was verified by measuring the mixtures in other two successive days. Thus, two similar calibration curves with sensitivities of 36 and 30 pA μL/ng were obtained. The sensitivities were quite similar in the three successive days. Furthermore, the reproducibility of the intercalator-based labeling reaction was also tested on a new Topas-microchip with new mixtures of ssDNA and MB. Thus, a new calibration plot was made obtaining a linear range comprised between 5 and 40 ng/μL with a sensitivity of 32 pA μL/ng ($r = 0.996$, $n = 5$).

The labeling reaction of the ssDNA with MB did not change with time; it took place immediately after mixing of ssDNA and MB. Thus, large incubation time was not necessary. When the signal of the mixture between MB (100 μM) and DNA (10 ng/μL) is tested during 3 h, the RSD for 15 measurements successively recorded is 2.8% with an average peak current of −0.45 nA (the RSD for the migration time is 1.2% with an average of 40.2 s). Similarly, for the mixture with a lower concentration of MB (50 μM) and the same of DNA (10 ng/μL) the RSD for ten measurements successively recorded along 2 h resulted to be 3.8% with an average peak current of −0.33 nA. In this case, RSD of the migration time is 1.3%(average of 39.8 s). Therefore, the good reproducibility of the microchip system and the labeling reaction has been also demonstrated for DNA analysis. Using DNA samples decreased the lifetime of the Topas microchips taken into account the previous work with this microchip material [33]. Partial adsorption of DNA could foul the channel surface decreasing the lifetime of microchip. In this case, microchips were employed during 75 runs without worsening of the analytical signals.

4 Concluding remarks

Electrochemical ssDNA detection in MCE through MB interaction is first reported herein. Firstly, different redox-active molecules have been evaluated for its use as DNA indicators on CE microchips. The organic dye MB has presented the best analytical signal by cyclic voltammetry. Thus, the reduction redox process of MB at −0.3 V has been studied and optimized on Topas-microchips with a homemade design that employs a gold wire-based detector.

Two end-channel detector designs have been developed for monitoring the MB reduction on Topas-microchips. The detector based on a 250 μm diameter gold wire has shown a high background current and noise level. This could be decreased by using 1-hexanethiol-modified gold wire electrode without worsening of the analytical signal.

The detector based on a guide channel, in which a 100 or 50 μm diameter gold wire is aligned accurately, has presented an excellent S/N. A small diameter produces a better isolation of the detector from the electric field. Furthermore, modification of these gold wire electrodes is not necessary because they presented a low background current and noise level.

The 100 μm diameter gold wire detector has been successfully employed in combination with Topas-microchips for the detection of ssDNA. An intercalator-based reaction has been achieved for labeling ssDNA using the organic dye MB for first time in microchips. Thus, the Topas-microchip with the amperometric detection has shown a good reproducibility for the free MB signal accomplishing a calibration plot based on the signal decrease upon the addition of ssDNA with a detection limit of 0.4 pg.

Work is in progress for sensitivity enhancement of the ED and achievement of the separation between single- and dsDNA.

This work has been supported by the FICYT under project IB05-151C2. Mario Castaño Álvarez thanks FICYT-Principado de Asturias for the award of a Ph.D. grant.

5 References

[1] Manz, A., Graber, N., Widmer, H. M., *Sens. Actuators B* 1990, *1*, 244–248.

[2] Manz, A., Harrison, D., Verpoorte, E., Fettinger, J. *et al.*, *J. Chromatogr.* 1992, *593*, 253–258.

[3] Li, S. F. Y., Kricka, L. J., *Clin. Chem.* 2006, *52*, 37–45.

[4] Muck, A., Jr., Wang, J., Jacobs, M., Chen, G. *et al.*, *Anal. Chem.* 2004, *76*, 2290–2297.

[5] Schöning, M. J., Jacobs, M., Muck, A., Knobbe, D.-T. *et al.*, *Sens. Actuators B* 2005, *108*, 688–694.

[6] Liu, Y., Ganser, D., Schneider, A., Liu, R. *et al.*, *Anal. Chem.* 2001, *73*, 4196–4201.

[7] Coltro, W. K. T., da Silva, J. A. F., da Silva, H. D. T., Richter, E. M. *et al.*, *Electrophoresis* 2004, *25*, 3832–3839.

[8] Liu, A. L., He, F. Y, Hu, Y. L, Xia, X. H., *Talanta* 2006, *68*, 1303–1308.

[9] Mela, P., van den Berg, A., Fintschenko, Y., Cummings, E. B. *et al.*, *Electrophoresis* 2005, *26*, 1792–1799.

[10] Castaño-Álvarez, M., Fernández-Abedul, M. T., Costa-García, A., *Electrophoresis* 2005, *26*, 3160–3168.

[11] Handal, M. I., Ugaz, V. M., *Expert Rev. Mol. Diagn.* 2006, *6*, 29–38.

[12] Chen, L., Ren, J., *Comb. Chem. High Throughput Screen.* 2004, *7*, 29–43.

[13] Liu, S., Guttman, A., *Trends Anal. Chem.* 2004, *23*, 422–430.

[14] Landers, J. P., *Anal. Chem.* 2003, *75*, 2919–2927.

[15] Tanyanyiwa, J., Abad-Villar, E. M., Fernández-Abedul, M. T., Costa-García, A. *et al.*, *Analyst* 2003, *128*, 1019–1022.

[16] Abad-Villar, E. M., Tanyanyiwa, J., Fernandez-Abedul, M. T., Costa-Garcia, A., Hauser, P.C., *Anal. Chem.* 2004, *76*, 1282–1288.

[17] Galloway, M., Stryjewski, W., Henry, A., Ford, S. M. *et al.*, *Anal. Chem.* 2002, *74*, 2407–2415.

[18] Galloway, M., Soper, S. A., *Electrophoresis* 2002, *23*, 3760–3768.

[19] Martin, R. S., Ratzlaff, K. L., Huyng, B. H., Lunte, S. M., *Anal. Chem.* 2002, *74*, 1136–1143.

[20] Castaño-Álvarez, M., Fernández-Abedul, M. T., Costa-García, A., *Anal. Bioanal. Chem.* 2005, *382*, 303–310.

[21] Lacher, N. A., Lunte, S. M., Martin, R. S., *Anal. Chem.* 2004, *76*, 2482–2491.

[22] Vickers, J., Henry, C. S., *Electrophoresis* 2005, *26*, 4641–4647.

[23] Woolley, A. T., Lao, K., Glazer, A. N., Mathies, R. A., *Anal. Chem.* 1998, *70*, 684–688.

[24] Keyton, R. S., Roussel, T. J., Jr., Crain, M. M., Jackson, D. J. *et al.*, *Anal. Chim. Acta* 2004, *507*, 95–105.

[25] Dawoud, A. A., Kawaguchi, T., Markushin, Y., Porter, M. D., Jankowiak, R., *Sens. Actuators B* 2006, *120*, 42–50.

[26] Yan, J. L., Du, Y., Liu, J. F., Cao, W. D. *et al.*, *Anal. Chem.* 2003, *75*, 5406–5412.

[27] Ertl, P., Emrich, C. A., Singhal, P., Mathies, R. A., *Anal. Chem.* 2004, *76*, 3749–3755.

[28] Hebert, N. R., Brazill, S. A., *Lab Chip* 2003, *3*, 241–247.

[29] Schwarz, M. A., Galliker, B., Fluri, K., Kappes, T., Hauser, P. C., *Analyst* 2001, *126*, 147–151.

[30] Liu, Y., Vickers, J. A., Henry, C. S., *Anal. Chem.* 2004, *76*, 1513–1517.

[31] Zeng, Y., Chen, H., Pang, D.-W., Wang, Z.-L., Cheng, J.-K., *Anal. Chem.* 2002, *74*, 2441–2445.

[32] Wang, Y., Chen, H., *J. Chromatogr. A* 2005, *1080*, 192–198.

[33] Castaño-Álvarez, M., Fernández-Abedul, M. T., Costa-García, A., *J. Chromatogr. A* 2005, *1109*, 291–299.

[34] Wang, J., Tian, B., Sahlin, E., *Anal. Chem.* 1999, *71*, 5436–5440.

[35] Wang, J., Mannino, S., Camera, C., Chatrathi, M. P. *et al.*, *J. Chromatogr. A* 2005, *1091*, 177–182.

[36] Kerman, K., Kobayashi, M., Tamiya, E., *Meas. Sci. Technol.* 2004, *15*, R1–R11.

[37] Kelley, S. O., Boon, E. M., Barton, J. K., Jackson, N. M., Hill, M. G., *Nucleic Acids Res.* 1999, *27*, 4830–4837.

[38] Boon, E. M., Ceres, D. M., Drummond, T. G., Hill, M. G., Barton, J. K., *Nat. Biotechnol.* 2000, *18*, 1096–1100.

[39] Hernández-Santos, D., González-García, M. B., Costa-García, A., *Anal. Chem.* 2005, *77*, 2868–2874.

[40] Hernández-Santos, D., Díaz-González, M., González-García, M. B., Costa-García, A., *Anal. Chem.* 2004, *76*, 6887–6893.

[41] Kerman, K., Ozkan, D., Kara, P., Meric, B. *et al.*, *Anal. Chim. Acta* 2002, *462*, 39–47.

[42] Wong, E. L. S., Gooding, J. J., *Anal. Chem.* 2003, *75*, 3845–3852.

[43] Palecek, E., Scheller, F., Wang, J. (Eds.), *Electrochemistry of Nucleic Acids and Proteins. Towards Electrochemical Sensors for Genomics and Proteomics*, Elsevier, Amsterdam 2005.

[44] Palecek, E., Fojta, M., *Anal. Chem.* 2001, *73*, 74A–84A.

[45] Marra, M. A., Jones, S. J. M., Astell, C. R., Holt, R. A. *et al.*, *Science* 2003, *300*, 1399–1404.

[46] Steenken, S., Jovanovic, S. V., *J. Am. Chem. Soc.* 1997, *119*, 617–618.

[47] Wong, E. L. S., Erohkin, P., Gooding, J. J., *Electrochem. Commun.* 2004, *6*, 648–654.

[48] Erdem, A., Kerman, K., Meric, B., Akarca, U. S., Ozsoz, M., *Anal. Chim. Acta* 2000, *422*, 139–149.

[49] Kara, P., Kerman, K., Ozkan, D., Meric, B. *et al.*, *Electrochem. Commun.* 2002, *4*, 705–709.

[50] Wang, B., Bouffier, L., Semeunynck, M., Mailley, P. *et al.*, *Bioelectrochemistry* 2004, *63*, 233–237.

[51] Carter, M. T., Rodriguez, M., Bard, A. J., *J. Am. Chem. Soc.* 1989, *111*, 8901–8911.

[52] Mahadevan, S., Palaniandavar, M., *Bioconjug. Chem.*, 1996, *7*, 138–143.

[53] Li, H., Xu, Z., Ji, L.-N., Li, W.-S., *J. Appl. Electrochem.* 2005, *35*, 235–241.

[54] Wang, S., Du, D., *Sensors* 2002, *2*, 41–49.

[55] Yang, W., Gooding, J. J., Hibbert, D. B., *J. Electroanal. Chem.* 2001, *516*, 10–16.

[56] Zeng, B., Yang, Y., Ding, X., Zhao, F., *Talanta* 2003, *61*, 819–827.

[57] Zhao, F., Zeng, B., Pang, D., *Electroanalysis* 2003, *15*, 1060–1066.

[58] Abad-Valle, P., Fernández-Abedul, M. T., Costa-García, A., *Biosens. Bioelectron.* 2007, *22*, 1642–1645.

[59] Castaño-Álvarez, M., Fernández-Abedul, M. T., Costa-García, A., *Ins. Sci. Technol.* 2006, *34*, 697–710.

[60] Jacobson, S. C., Hergenroder, R., Koutny, L.B., Warmack, R.J., Ramsey, J. M., *Anal. Chem.* 1994, *66*, 1107–1113.

[61] Rye, H. S., Yue, S., Wemmer, D. E., Quesada, M. A. *et al.*, *Nucleic Acids Res.* 1992, *20*, 2803–2812.

[62] Jurado, E., Fernández-Serrano, M., Nuñez-Olea, J., Luzón, G., Lechuga, M., *Chemosphere* 2006, *65*, 278–285.

[63] Tuite, E., Norden, B., *J. Am. Chem. Soc.* 1994, *116*, 7548–7556.

